Hybridized Nondegenerate 6*d* and 5*f* Virtual-Bound-States Model for Actinides Metals *

R. Jullien, E. Galleani d'Agliano, † and B. Coqblin
Laboratoire de Physique des Solides, ‡ *Faculté des Sciences, 91—Orsay, France*
(Received 19 October 1971; revised manuscript received 27 December 1971)

A simple model taking into account two hybridized and nondegenerate 6*d* and 5*f* virtual bound states is presented here for describing the properties of pure actinide metals. The model which describes the *d-f* hybridization by a simple mixing one-body Hamiltonian is treated in the usual Hartree-Fock self-consistent scheme of Friedel-Anderson. The model can be made consistent with previous band calculations and with specific-heat measurements giving a large density of states at the Fermi level. It can then account for the absence of localized magnetism for the strongly *d-f* hybridized uranium, neptunium, and plutonium metals and for the occurrence of magnetism only in the middle of the series for curium and berkelium.

I. EXPERIMENTAL INTRODUCTION

The present state of understanding of the magnetism of pure actinides has greatly increased in recent years.[1-5] Actinides are characterized by the filling up of the 5*f* shell, while the 6*d* band is occupied by one to three electrons and the 7*s* band contains roughly two electrons. Actinides seem like rare earths at first sight, but in fact the 5*f* electrons are less localized than the 4*f* electrons in rare earths and cannot be treated independently of the 6*d* and 7*s* electrons.

The plot of the atomic volume of actinides[6,7] along the series allows us to make a first classification. As shown in Fig. 1, actinium and thorium have almost the same atomic volume as the corresponding lanthanides. But then from proactinium to plutonium the atomic volume has values intermediate between those of rare earths and those of 4*d* or 5*d* transition metals, the values being closer to those of transition elements. The atomic radius increases for americium and lies very close to the corresponding trivalent rare earth, and, at last, curium and berkelium in its fcc phase, [8] have atomic volumes similar to those of trivalent rare earths.

We will now review the different properties of actinides. Francium and radium are normal metals with one or two electrons in their 7*s* band. Actinium is very similar to lanthanum with a $7s^2 6d^1$ configuration and a valence equal to 3. Thorium has a valence equal to 4 and roughly the atomic configuration $7s^2 6d^2$. In metallic thorium the 5*f* character is negligible,[9] while the 6*d* character begins to be pronounced enough to give rise to a narrow band with essentially a 6*d* character.[6] The electronic constant γ of the specific heat is of the order 4.5 mJ/mole °K^2, giving a density of states of ~1 state/eV atom for one spin direction characteristic of transition elements. Thorium is also a regular BCS superconductor with a transition temperature equal to 1.33 °K at normal pressure,[2,10] which does not change very much with pressure.[11] It seems that the 5*f* character appears around proactinium and uranium and increases regularly along the series according to the plot of the atomic volume and to the specific heat[1] and magnetic susceptibility[3] measurements which give the total density of states.

The electronic constant γ of the specific heat is found to be between 9 and 12 mJ/mole °K^2, giving rise to a 2-states/eV-atom (for one-spin direction) density of states for uranium metal. The constant γ is larger for neptunium, i.e., roughly 14 mJ/mole °K^2, which gives a 3-states/eV-atom (for one-spin direction) density of states. The values of γ for plutonium are very spread out[1] because of the experimental difficulties: They are mostly around 14–15 mJ/mole °K^2, giving a 3-states/eV-atom density of states, but much larger values are found for both regular plutonium and ^{242}Pu isotope[12] samples.

The magnetic susceptibility of actinide metals has been measured from low temperatures to room temperature, and all metals from proactinium to plutonium have a temperature-independent magnetic susceptibility, indicating that there is no appreciable localized magnetic moment as shown in Fig. 2.[3] In the peculiar case of plutonium, there was a long controversy on the possibility of a small magnetic moment. The resistivity measurements on α-Pu single crystals[13] do not show any sharp transitions as are found in rare-earth single crystals near their magnetic transitions. Furthermore, measurements of the differential susceptibility show that the upper limit of a net magnetic moment must be dropped to around $0.01\,\mu_B$/Pu atom.[3] The lack of a localized moment at the plutonium nucleus is found by Mössbauer work on[3] α-^{242}Pu and NMR work on δ-Pu.[14] It now seems well established that plutonium has no localized moment. The magnetic susceptibility χ is equal to 2.7×10^{-4} emu/mole for Pa,[15] 3.8×10^{-4} emu/mole for α-U,[16] 5.6×10^{-4} emu/mole for α-Np,[3] and 5.1

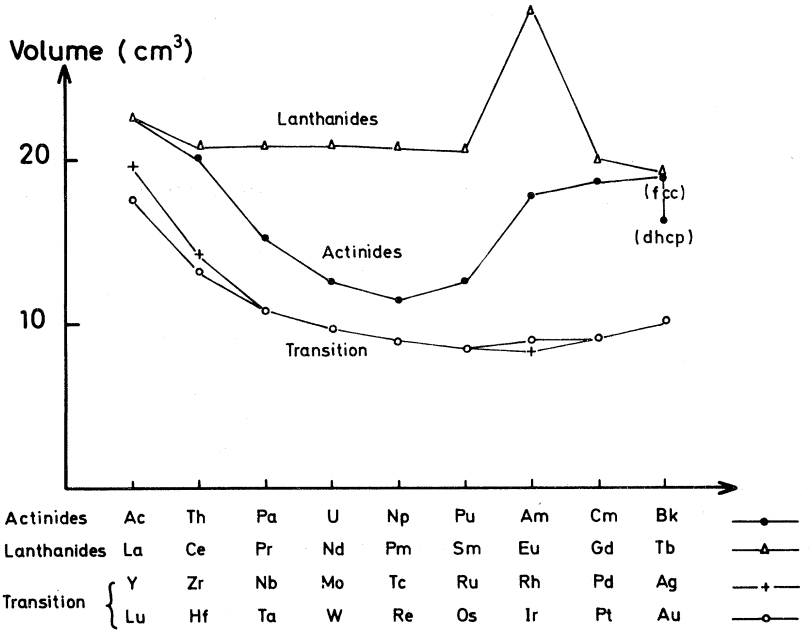

FIG. 1. Plot of the molar volume (in cm^3) for the actinide series compared with lanthanide, 4*d* and 5*d* series.

$\times 10^{-4}$ emu/mole for α-Pu.[13] In spite of possible exchange-enhancement effects for the magnetic susceptibility, we can have an idea of the density of states by assuming that χ is a simple Pauli paramagnetic susceptibility. The corresponding density of states is 4.1 states/eV atom (for one-spin direction) for Pa, 5.8 for α-U, 8.6 for α-Np, and 8.1 for α-Pu.

All the metals from proactinium to plutonium are characterized by a very large density of states coming from the specific-heat data and checked by the magnetic susceptibility data. The density of states is too large to be attributed only to a simple 6*d* character, and the absence of magnetism shows that the 5*f* bands are certainly much broader than in rare-earth metals. Moreover, we can show that, with the 6*d* and 5*f* wave functions used for describing actinides, there results a strong hybridization between the 6*d* and 5*f* electrons.[6,17] It has been previously proposed that at least proactinium, uranium, neptunium, and pultonium have a complex band structure with a strongly hybridized *d* and *f* character. An estimate of the hybridization can be found in the computed value by band calculations of the width of the "*f* band," which is more exactly the width of the *f* band hybridized with *d* band. It varies along the actinide series, going from 2.7 eV for β-Pa and 3 eV for U to 1.3 eV for Pu and 0.7 eV for γ-Am and γ-Cm.[18]

The small 5*f* character of proactinium and uranium can also be seen from their peculiar superconducting properties. The superconductivity of proactinium is not definitively established. Some authors[2,5] found it superconducting below 1.4 °K, however, recent experiments showed no sign of becoming superconducting in the resistivity measurements down to 0.93 °K, nor using a magnetic method down to 0.89 °K.[19] Uranium-α seems now to be not a bulk superconductor at normal pressure but superconductivity appears when pressure is applied. The transition temperature increases rap-

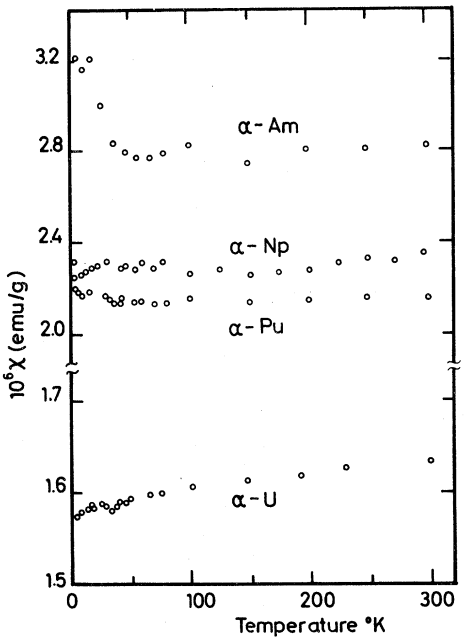

FIG. 2. Magnetic susceptibility (in 10^{-6} emu/g) vs temperature for α-U, α-Pu, α-Np, and α-Am elements (after Brodsky, Ref. 3).

idly with pressure, reaching around 2 °K between 10 and 20 kbar, according to the results of Gardner and Smith.[20] Moreover, the electronic specific-heat constant increases rapidly under a 10-kbar pressure.[21]

The behavior of actinides changes completely at americium as shown on Fig. 1. The valence of americium is not definitively established, but it is sure that the valence, which is equal to 5 or 6 for neptunium and plutonium, becomes smaller for americium. From Fig. 1, the value of atomic volume for americium gives a valence close to 3 in spite of previous investigation of Zachariasen[22] and Matthias *et al.*[23] The heat of vaporization,[24] vapor pressure,[24] and compressibility[25] of americium may be interpreted as indicating that it is more likely to be trivalent. Moreover, americium, as well as curium[26,27] and one phase of berkelium,[8] has the double hexagonal-close-packed structure, which is also found in the beginning of the series of trivalent rare earths. So, it is more convincing to follow Hill[2] and adopt a valence close to 3 for americium. The magnetic susceptibility of americium is constant above 100 °K and increases below[3] 100 °K; but this low-temperature-dependent susceptibility is probably due to neptunium magnetic impurities.[3,28] Its value is 6.7×10^{-4} emu/mole and corresponds to a density of states of 10.3 states/eV atom. So americium has no magnetic localized moment, but the question of its magnetism is not perfectly clear. It can be either a Pauli paramagnet or a Van Vleck paramagnet if its valence is strictly 3, leading to the $5f^6$ configuration. According to McWhan,[29,30] americium would be a Van Vleck paramagnet with a $J=0$ ground state separated from an excited $J=1$ state by 3.000 °K.

The elements after americium are magnetic and are very close to the trivalent rare earths according to Fig. 1. From Bansal,[15] curium follows a Curie-Weiss law with an effective magnetic moment ranging from 7.97 to 8.1μ_B with a negative Curie temperature of order − 350 °K. Marei[7] has also found that curium follows a Curie-Weiss law with an effective moment of order of 8μ_B and with a Curie temperature of order of − 300 °K. It is interesting to note on the plots of Marei[7] that the magnetic susceptibility follows the Curie-Weiss law at high temperatures and begins to depart from this law around 200 °K. The nature of ordering is not established for curium at low temperatures, although the negative Curie temperature indicates an antiferromagnetic ordering. Although the Curie temperature is large and negative, and consequently the meaning of Curie-Weiss law is not very clear, the 8μ_B effective moment found experimentally is remarkably close to the theoretical value of the $5f^7$ configuration. So the experiments of Bansal and Marei[7] indicated that curium is a magnetic actinide with a valence equal to 3 and a $5f^7$ configuration as for gadolinium.

Berkelium has been studied recently by Peterson *et al.*[8] All samples exhibit a face-centered-cubic phase with a lattice parameter of 5 Å. In addition, several samples exhibited a double hexagonal-close-packed phase with lattice parameters of $a=3.42$ Å and $c=11.07$ Å. Present data indicate that the fcc phase is the high-temperature phase with respect to the double hcp (dhcp) phase. The corresponding molar volumes are 18.8 cm^3 for the fcc phase and 16.2 cm^3 for the dhcp phase; the atomic volume is roughly 14% smaller for the dhcp phase than for the fcc phase. So the valences of the two phases are different. The method of Zachariasen[22] gives a valence of 3.5 for fcc and 3.9 for dhcp.[8] These values are overestimated because the method of Zachariasen starts from thorium for determining the valences. On the other hand, the method of Cunningham and Wallmann[26] yields values of 2.8 for fcc valence and 3.2 for dhcp valence,[8] but these values are underestimated because the method of Cunningham and Wallmann starts from curium for determining the valences. Another way of determining their valences is to compare the atomic volumes of actinides with those of the corresponding rare earths. Since the atomic volume of fcc Bk is the same as that of terbium, we can attribute a valence equal to 3 for fcc Bk. Since the variation of volume is of order 25–30% between trivalent cerium and tetravalent cerium or between divalent and trivalent europium and ytterbium, we can attribute a valence equal to approximately 3.5 to dhcp Bk. Consequently, the magnetic moments of the two berkelium phases should be different with a larger magnetic moment for the fcc phase than for the dhcp phase. This difference cannot be seen clearly on the experimental results of magnetic susceptibility, because the samples are generally made of admixtures of fcc and dhcp phases and also because the samples contain large amounts of californium, the next element after berkelium.[8] However, on a first sample containing fcc phase and a large amount of californium, the magnetic susceptibility follows a Curie-Weiss law with an effective magnetic moment of 8.23μ_B and a positive Curie temperature of 64 °K. At 140 °K, Bk begins exhibiting ferromagnetic ordering. In the two other samples containing the two phases, a Curie-Weiss law is observed with an effective magnetic moment of 8.52μ_B or 8.83μ_B and a negative Curie temperature of − 72 or − 33 °K; at low temperatures, the magnetic susceptibility departs from a Curie-Weiss law to exhibit a transition for antiferromagnetism. So we can conclude that the magnetic moment of berkelium metal is of order 8.5μ_B, relatively close to the theoretically expected value for the f^8 configuration as terbium in the rare-

earth series; but we cannot conclude on the difference between magnetic moments of the two phases. Therefore, berkelium is a magnetic actinide with an fcc phase close to the trivalent magnetic f^8 configuration of rare earths. Moreover, there is an interesting phase transformation accompanied by a valence charge, the phase with the smallest valence existing at the highest temperatures, as, for example, in cerium. The transition with a valence change in berkelium would be obviously very interesting to study experimentally in detail.

Experimentally, we can distinguish three groups in the actinides series, as previously predicted by Friedel.[6] (i) Transition metals with a pronounced $6d$ character and a negligible $5f$ character: This is the case of actinium and thorium, which is superconducting. (ii) Mixed $6d$-$5f$ metals with a hybridized d-f character and with a valence around 5: This is the case of proactinium, uranium, neptunium, and plutonium, which are not magnetic and have a large density of states at the Fermi level. (iii) Rare-earth metals with highly localized $5f$ electrons and a valence close to 3: This is the case of americium, curium, and fcc berkelium, and the last two have magnetic moments corresponding roughly to the $5f^7$ and $5f^8$ configurations, respectively.

II. THEORETICAL MODEL

The purpose of this paper is essentially to explain the absence of localized magnetism for actinides before curium by taking into account a strong hybridization between $6d$ and $5f$ electrons and consequently to account for the experimentally observed "delay" for the occurrence of magnetism appearing in actinides by comparison with rare earths.

In actinide metals, the $5f$ wave functions are not very localized; consequently, there results an important overlap between two $5f$ wave functions centered on two neighboring sites and as a result a $5f$ band with an appreciable width, in contrast with the situation of rare earths. Both $5f$ and $6d$ electrons are able to form bands in actinides, and the hybridization comes from the asymmetric bondings between $5f$ and $6d$ electrons.[6,17] Many band calculations have been done in actinide metals and compounds and are able to predict, in some cases, the shape of the density of states.

Kmetko and Hill[18] have deduced from nonrelativistic band calculations an order of magnitude for the half-width of the "hybridized $5f$ band" in actinides, as shown in Fig. 3. The half-width goes through a maximum of order 1.5 eV at uranium, where there is a very strong d-f hybridization, and then decreases till a small value of order 0.35 eV for americium and curium, where the hybridization is certainly very small. Band calculations of actinides have also been performed by use of a symmetrized relativistic augmented-plane-wave (APW) method, and substantial differences have been found with respect to the nonrelativistic calculations concerning the relative position of the different bands.[31,32] Anyway, the magnitude of the hybridized $5f$ bandwidth, which we can roughly estimate from the region of "$5f$ asymptotes," where APW calculations are inaccurate, follows qualitatively the same curve as that shown in Fig. 3. For example, the region of "$5f$ asymptotes" is of order 1.3 eV in thorium, 2 eV in uranium, and split in two regions of 0.5-eV width in plutonium, while the d-f hybridization is, in any case, very small in americium and curium. However, as pointed out by Freeman and Koelling,[32] the APW calculations are in fact inaccurate in describing the narrow $5f$ bands and cannot explain at all the occurrence of magnetism. So, in spite of the band character of the d and f electrons, we adopt, for describing essentially the magnetic properties of actinides, an opposite point of view which is better for the description of magnetism and easier to handle mathematically. The three main assumptions of the theoretical model are the following.

(i) We treat the one-impurity problem. This means that we consider all the atoms forming the actinide metal as independent impurities and that we start from $6d$ and $5f$ localized levels for each atom.[33]

(ii) We treat the $6d$ and $5f$ localized levels by the resonant scattering mechanism. This means that we have two virtual bound states in resonance with a broad $7s$ band. We neglect the orbital degeneracy and the spin-orbit coupling in this first paper, and we treat the two virtual bound states in the usual Friedel-Anderson[34-36] framework using the Hartree-Fock approximation.

(iii) We treat the d-f hybridization by taking in this first paper the simple phenomenological one-

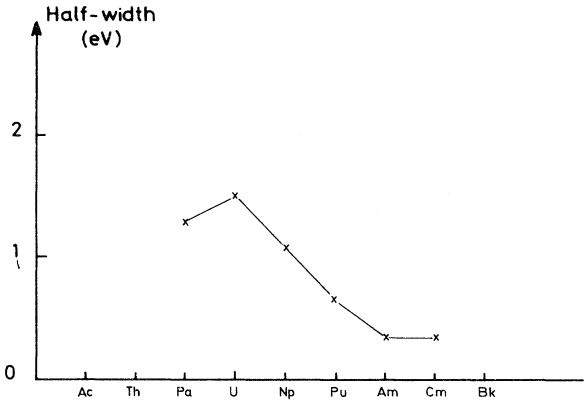

FIG. 3. Plot in eV along the actinide series of the "hybridized f half-width" given by the band calculations of Kmetko and Hill (Ref. 18).

body mixing interaction term between 6d and 5f electrons exactly as the mixing term used by Anderson[36] for describing d virtual bound states.

Obviously, this simple model will not be valid for describing band properties of actinides such as transport properties or, for example, the effective mass of d and f electrons, but it could account fairly well for the magnetic properties of actinides and especially for the occurrence of localized magnetism. Another trouble will certainly come from the Lorentzian form of the densities of states which deeply overestimates the tails of the band, especially for the d band. The validity of such a model will be discussed in Sec. V when comparing our results to the experimental data of pure actinides. A first short account on this model has already been presented.[37]

The Hamiltonian we use here is a natural extension of the Anderson Hamiltonian[36] to the case of two d and f virtual bound states with hybridization and can be written

$$H = H_0 + H_1 + H_2 + H_3 \ . \tag{1}$$

(i) The H_0 term represents the kinetic energy of the conduction electrons coming from the 7s band and of the localized electrons coming from the 6d and 5f levels:

$$H_0 = \sum_{k,\sigma} \epsilon_k c^*_{k\sigma} c_{k\sigma} + E_d^{(0)} \sum_{\sigma} c^*_{d\sigma} c_{d\sigma} + E_f^{(0)} \sum_{\sigma} c^*_{f\sigma} c_{f\sigma} \ . \tag{2}$$

We use the usual notations of Anderson.[36] $E_d^{(0)}$ is the position of the unperturbed d level, and $E_f^{(0)}$ is the position of the unperturbed f level.

(ii) The H_1 term represents the resonant scattering interactions with the conduction band and is given by simple one-body mixing terms:

$$H_1 = \sum_{k,\sigma} (V_{kd} c^*_{k\sigma} c_{d\sigma} + V^*_{kd} c^*_{d\sigma} c_{k\sigma}) + \sum_{k,\sigma} (V_{kf} c^*_{k\sigma} c_{f\sigma} + V^*_{kf} c^*_{f\sigma} c_{k\sigma}) . \tag{3}$$

(iii) The H_2 term represents the part of the two-body correlations between d and f electrons which will give a nonzero result in the usual Hartree-Fock approximation, i.e., the approximation which takes an average value over the occupation number of d and f levels. So the H_2 term takes into account the Coulomb repulsion between d electrons, between f electrons, between a d and f electron, and the exchange interaction between a d and f electron. With the usual notations $n_{d\sigma}$ and $n_{f\sigma}$, the H_2 term is expressed as

$$H_2 = U_{dd} n_{d\uparrow} n_{d\downarrow} + U_{ff} n_{f\uparrow} n_{f\downarrow} + U_{df} (n_{d\uparrow} n_{f\downarrow} + n_{d\downarrow} n_{f\uparrow}) + (U_{df} - J_{df})(n_{d\uparrow} n_{f\uparrow} + n_{d\downarrow} n_{f\downarrow}) \ . \tag{4}$$

The parameters U_{dd}, U_{ff}, U_{df}, and J_{df} are given by the following integrals:

$$\begin{aligned} U_{dd} &= \int\int |\phi_d(\vec{r}_1)|^2 (e^2/r_{12}) |\phi_d(\vec{r}_2)|^2 d\vec{r}_1 d\vec{r}_2 \ , \\ U_{ff} &= \int\int |\phi_f(\vec{r}_1)|^2 (e^2/r_{12}) |\phi_f(\vec{r}_2)|^2 d\vec{r}_1 d\vec{r}_2 \ , \\ U_{df} &= \int\int |\phi_d(\vec{r}_1)|^2 (e^2/r_{12}) |\phi_f(\vec{r}_2)|^2 d\vec{r}_1 d\vec{r}_2 \ , \\ J_{df} &= \int\int \phi^*_d(\vec{r}_1) \phi^*_f(\vec{r}_2) (e^2/r_{12}) \phi_d(\vec{r}_2) \phi_f(\vec{r}_1) d\vec{r}_1 d\vec{r}_2 \ . \end{aligned} \tag{5}$$

(iv) The H_3 term is introduced for describing the d-f hybridization in a phenomenological way by a one-body mixing term:

$$H_3 = \sum_{\sigma} (V_{df} c^*_{d\sigma} c_{f\sigma} + V^*_{df} c^*_{f\sigma} c_{d\sigma}) \ . \tag{6}$$

At last, to solve the Hamiltonian (1), we use, in addition to the Hartree-Fock approximation for (4), two other simplifying approximations.

(i) Since we do not know precisely the relative values of the four parameters entering (4), we make the approximation which takes all the parameters of the Coulomb and exchange interaction equal to each other:

$$U_{dd} = U_{ff} = U_{df} = J_{df} = U \ . \tag{7}$$

The approximation (7) overestimates the value of J_{df} and treats equally the d and f electrons, which in fact corresponds to an overestimation of the d-electron contribution. This approximation, which simplifies a little the calculations, is used here because we do not know the precise values of the different parameters U_{dd}, U_{ff}, U_{df}, and J_{df}. However, we can justify the different terms of the approximation (7) as follows: A precise knowledge of the exchange integral J_{df} compared to the Coulomb integral U_{df} should be crucial if the two d and f levels were "degenerate"[33] or close to each other. On the contrary, in the physical case of actinides described here, the two levels are well separated from each other, so that the rough evaluation of J_{df} made in (7) can be considered as a not too bad approximation.

On the other hand, the second part of the approximation $U_{dd} = U_{ff} = U_{df}$, which corresponds to an overestimation of the d contribution, is not too critical and does not affect deeply the physical results, because the average value $\langle n_{d\sigma} \rangle$ of the d occupation number is always relatively small compared to 1 in the present physical case.

With the approximation (7), the Hamiltonian (4) can be simply written

$$H_2 = U(n_{d\uparrow} + n_{f\uparrow})(n_{d\downarrow} + n_{f\downarrow}) \ . \tag{8}$$

(ii) The second approximation is to assume that the V_{df} term entering (6) is constant, independent of the spin and also of the relative positions of the d and f virtual bound states. We will discuss the validity of such an approximation in the Conclusion.

III. MATHEMATICAL TREATMENT

We treat the Hamiltonian (1) by the same method as Anderson[36] at zero temperature. The Green's

function $\hat{G}(E)$ for zero temperature is defined by

$$\lim(E+is-H)\hat{G}(E)=1 \quad \text{as } s\to 0^+ . \tag{9}$$

The system of equations for the matrix elements of the Green's function is, in the Hartree-Fock approximation,

$$\begin{aligned}
&(E+is-E_f^\sigma)G_{ff}^\sigma(E)-\textstyle\sum_k V_{fk}G_{kf}^\sigma(E)-V_{fd}G_{df}^\sigma(E)=1 ,\\
&(E+is-E_d^\sigma)G_{df}^\sigma(E)-\textstyle\sum_k V_{dk}G_{kf}^\sigma(E)-V_{df}G_{ff}^\sigma(E)=0 ,\\
&(E+is-\epsilon_k)G_{kf}^\sigma(E)-V_{kd}G_{df}^\sigma(E)-V_{kf}G_{ff}^\sigma(E)=0 .
\end{aligned} \tag{10}$$

The system of equations for $G_{dd}^\sigma(E)$, $G_{kd}^\sigma(E)$, and $G_{fd}^\sigma(E)$ is obtained from (10) by permuting the index d and f.

In Eqs. (10), we have introduced the new energies for the d and f levels:

$$\begin{aligned}
E_d^\sigma &= E_d^{(0)}+U_{dd}\langle n_{d-\sigma}\rangle+U_{df}\langle n_{f-\sigma}\rangle+(U_{df}-J_{df})\langle n_{f\sigma}\rangle ,\\
E_f^\sigma &= E_f^{(0)}+U_{ff}\langle n_{f-\sigma}\rangle+U_{df}\langle n_{d-\sigma}\rangle+(U_{df}-J_{df})\langle n_{d\sigma}\rangle ,
\end{aligned} \tag{11}$$

which, in the approximation (7), are simply functions of the total number of d and f electrons for a given spin σ:

$$\begin{aligned}
E_d^\sigma &= E_d^{(0)}+Un_{-\sigma} ,\\
E_f^\sigma &= E_f^{(0)}+Un_{-\sigma} ,
\end{aligned} \tag{12}$$

with

$$n_\sigma = n_{d\sigma}+n_{f\sigma} . \tag{13}$$

In (12) and in (13), we have omitted the average symbols $\langle\cdots\rangle$ for $\langle n_{d\sigma}\rangle$ and $\langle n_{f\sigma}\rangle$. We will do so also in the following.

In solving Eq. (10), we write

$$\lim_{s\to 0^+}\sum_k \frac{|V_{dk}|^2}{E+is-\epsilon_k}=-i\Gamma_d ,$$

$$\lim_{s\to 0^+}\sum_k \frac{|V_{fk}|^2}{E+is-\epsilon_k}=-i\Gamma_f , \tag{14a}$$

$$\lim_{s\to 0^+}\sum_k \frac{V_{dk}V_{fk}}{E+is-\epsilon_k}=0 , \tag{14b}$$

where Γ_d and Γ_f are the classical half-widths of the d and f virtual bound states and are given by

$$\begin{aligned}
\Gamma_d &= \pi\langle|V_{dk}|^2\rangle\rho_s(E_F) ,\\
\Gamma_f &= \pi\langle|V_{fk}|^2\rangle\rho_s(E_F) ,
\end{aligned} \tag{15}$$

where $\rho_s(E_F)$ is the density of states of the conduction band, which is assumed to be constant, and E_F is the Fermi energy.

In the expressions (14a), we have neglected, as usual,[36] the real part which corresponds simply to an energy shift. In the expression (14b), we have taken a potential with a spherical symmetry which leads to zero value for the integral (14b), because the angular parts of V_{kf} and V_{kd} are thus proportional to spherical harmonics of different l values and consequently orthogonal.

At last, the diagonal matrix elements for $\hat{G}(E)$ are given by

$$\begin{aligned}
G_{dd}(E) &= \frac{E-E_f^\sigma+i\Gamma_f}{(E-E_f^\sigma+i\Gamma_f)(E-E_d^\sigma+i\Gamma_d)-|V_{df}|^2} ,\\
G_{ff}(E) &= \frac{E-E_d^\sigma+i\Gamma_d}{(E-E_d^\sigma+i\Gamma_d)(E-E_f^\sigma+i\Gamma_f)-|V_{df}|^2} .
\end{aligned} \tag{16}$$

The extra density of states coming from d and f states is given by

$$\begin{aligned}
\rho_\sigma(E) &= \rho_{d\sigma}(E)+\rho_{f\sigma}(E)\\
&= -(1/\pi)\,\mathrm{Im}\,[G_{dd}^\sigma(E)+G_{ff}^\sigma(E)] .
\end{aligned} \tag{17}$$

In the simple case $V_{df}=0$, we find

$$\rho_\sigma(E)=\frac{1}{\pi}\left(\frac{\Gamma_f}{(E-E_f^\sigma)^2+\Gamma_f^2}+\frac{\Gamma_d}{(E-E_d^\sigma)^2+\Gamma_d^2}\right). \tag{18}$$

The expression (18) is the sum of two Lorentzians centered on E_d^σ and E_f^σ with half-widths Γ_d and Γ_f, which corresponds to the trivial extension of the Anderson result to the case of two virtual bound states which do not interact with each other.

In the general case $V_{df}\neq 0$, the expression of $\rho_\sigma(E)$ takes also the form of a sum of two Lorentzians:

$$\rho_\sigma(E)=\frac{1}{\pi}\left(\frac{\Gamma_1}{(E-E_1^\sigma)^2+\Gamma_1^2}+\frac{\Gamma_2}{(E-E_2^\sigma)^2+\Gamma_2^2}\right). \tag{19}$$

The centers E_1^σ and E_2^σ and the two half-widths Γ_1 and Γ_2 are the real parts and the opposite of the imaginary parts of the poles of the Green's-function (16) solutions of the equation

$$\begin{aligned}
E^2-E(E_d^\sigma-i\Gamma_d+E_f^\sigma-i\Gamma_f)\\
+(E_f^\sigma-i\Gamma_f)(E_d^\sigma-i\Gamma_d)-|V_{df}|^2=0 .
\end{aligned} \tag{20}$$

The values of E_1^σ and E_2^σ are given by

$$\begin{aligned}
E_1^\sigma &= \tfrac{1}{2}(E_d^\sigma+E_f^\sigma)+\tfrac{1}{2}\epsilon[\tfrac{1}{2}(|z|+\mathrm{Re}z)]^{1/2} ,\\
E_2^\sigma &= \tfrac{1}{2}(E_d^\sigma+E_f^\sigma)-\tfrac{1}{2}\epsilon[\tfrac{1}{2}(|z|+\mathrm{Re}z)]^{1/2} .
\end{aligned} \tag{21}$$

The values of Γ_1 and Γ_2 are given by

$$\begin{aligned}
\Gamma_1 &= \tfrac{1}{2}(\Gamma_d+\Gamma_f)-\tfrac{1}{2}[\tfrac{1}{2}(|z|-\mathrm{Re}z)]^{1/2} ,\\
\Gamma_2 &= \tfrac{1}{2}(\Gamma_d+\Gamma_f)+\tfrac{1}{2}[\tfrac{1}{2}(|z|-\mathrm{Re}z)]^{1/2} ,
\end{aligned} \tag{22}$$

where $|z|$ and $\mathrm{Re}z$ are the modulus and the real part of the complex number z:

$$\begin{aligned}
z=(E_d^\sigma-E_f^\sigma)^2-(\Gamma_d-\Gamma_f)^2+4|V_{df}|^2\\
-2i(\Gamma_d-\Gamma_f)(E_d^\sigma-E_f^\sigma) ,
\end{aligned} \tag{23}$$

and $\epsilon=\pm 1$ has the same sign as the imaginary part of z, i. e., $-2(\Gamma_d-\Gamma_f)(E_d^\sigma-E_f^\sigma)$.

In order to write (22), we had previously remarked that, in the approximation (7) used here, Γ_1 and Γ_2 are independent of n_σ and consequently of the spin σ, because Γ_1 and Γ_2 depend only on the difference $E_f^\sigma-E_d^\sigma$. Moreover, E_1^σ and E_2^σ depend on

$n_{-\sigma}$ only by the first factor $\frac{1}{2}(E_d^\sigma + E_f^\sigma)$ in (21), and we can write

$$E_1^\sigma = E_1^{(0)} + Un_{-\sigma}\,, \qquad E_2^\sigma = E_2^{(0)} + Un_{-\sigma}\,. \tag{24}$$

$E_1^{(0)}$ and $E_2^{(0)}$ are functions of $E_d^{(0)}$ and $E_f^{(0)}$ by the same expressions (21) as E_1^σ and E_2^σ are functions of E_d^σ and E_f^σ.

The effect of d-f hybridization is easy to see on the density of states. For $V_{df}=0$, we have obviously $E_1^\sigma = E_f^\sigma$, $E_2^\sigma = E_d^\sigma$, $\Gamma_1 = \Gamma_f$, and $\Gamma_2 = \Gamma_d$. When $|V_{df}|^2$ increases from a zero value, the two centers E_1^σ and E_2^σ are "pushed away" from each other and the two widths Γ_1 and Γ_2 become more and more "equal." This effect can be observed in Fig. 4, showing the density of states for a typical set of parameters U, Γ_d, Γ_f, E_f^σ, E_d^σ, and increasing V_{df} values.

The main physical effect is essentially the variation of the two widths when V_{df} increases. In particular, if we take two Lorentzians with Γ_f much smaller than Γ_d, which will physically correspond to the case of actinides as discussed later, the hybridization drastically increases the narrowest Lorentzian. It is consequently easy to predict right now that magnetism will be more difficult to obtain in the presence of the d-f hybridization. In fact, we have started from this physical idea to build up the model used here, because the d character and consequently the d-f hybridization are certainly more important for actinides than for rare earths.

A more quantitative idea of the effect of the hybridization is shown in Fig. 5, where we have plotted Γ_1 and Γ_2 vs $E_f^{(0)} - E_d^{(0)}$ for different values of V_{df} and for $\Gamma_d = 10\Gamma_f$. The effect of hybridization is more important when the two levels are

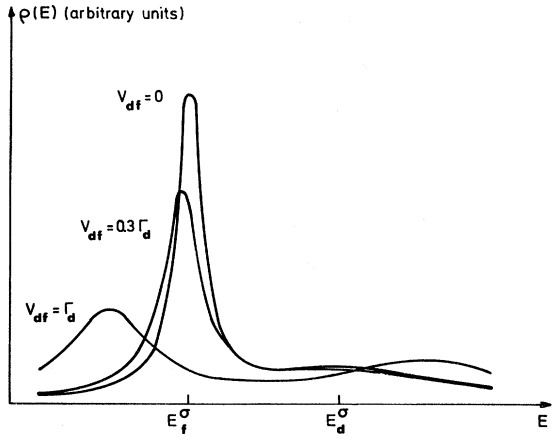

FIG. 4. Theoretical d and f extra density of states for a typical set of parameters $\Gamma_d = 10\ \Gamma_f$, $E_d^{(0)} - E_f^{(0)} = \Gamma_d$, and three different values of $V_{df} = 0,\ 0.3\ \Gamma_d,\ \Gamma_d$, which show the effect of the hybridization.

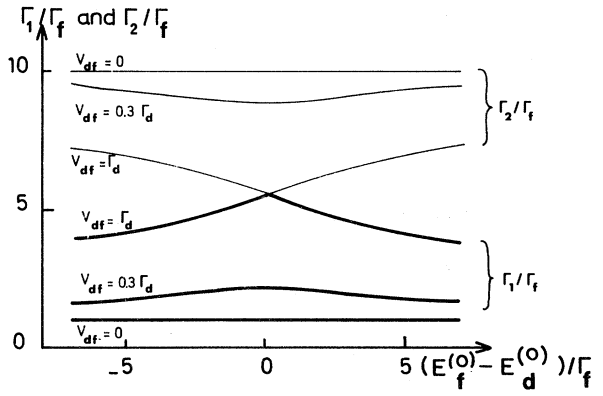

FIG. 5. Plot of Γ_1/Γ_f (thick line) and Γ_2/Γ_f (thin line) vs $(E_f^{(0)} - E_d^{(0)})/\Gamma_f$ for $\Gamma_d = 10\ \Gamma_f$ and three different values of $V_{df} = 0,\ 0.3\ \Gamma_d,\ \Gamma_d$.

closer to each other. So, when the 5f character increases, as is the case along the actinide series, the width Γ_1 of the narrowest level, or the width of the "hybridized f band," increases first, goes through a maximum when $E_f^{(0)} = E_d^{(0)}$, and then decreases to reach Γ_f when the 5f level is very much occupied. When the hybridization is not too large, i.e., $V_{df} < \frac{1}{2}(\Gamma_d - \Gamma_f)$, the values of Γ_1 and Γ_2 for $E_f^{(0)} = E_d^{(0)}$ are different, as is shown in Fig. 5 for $V_{df} = 0.3\Gamma_d$. On the contrary, when the hybridization is large, i.e., $V_{df} > \frac{1}{2}(\Gamma_d - \Gamma_f)$, the values of Γ_1 and Γ_2 for $E_f^{(0)} = E_d^{(0)}$ are equal, as is shown in Fig. 5 for $V_{df} = \Gamma_d$. Moreover, the more the V_{df} value is large, the more the relative variation of Γ_1 is important. The theoretical Fig. 5 can be related to the Fig. 3, in order to make consistent the model with the results of band calculations and consequently to have an estimate of the values of the parameters involved in the theoretical model.

We think that the V_{df} value is large, if we consider, in Fig. 3, the rapid decrease of the band half-width between its maximum at uranium and its value for americium and curium. However, this feature can be considered only as a tentative indication rather than a definite proof for a large V_{df} value, and, in fact, we will prefer to deduce the large value of the hybridization in actinides from their magnetic properties, as will be discussed later on. Furthermore, the values of Γ_d and Γ_f can be estimated by comparison with Fig. 3 in the following way: The maximum value $\frac{1}{2}(\Gamma_d + \Gamma_f)$ of Γ_1 corresponds to the uranium band half-width, which is of order 1.5 eV, while the limiting value Γ_f of Γ_1 when there is no longer any hybridization is probably very close to the americium band half-width, which is equal to 0.35 eV in Fig. 3. So we deduce that the ratio Γ_d/Γ_f is of order 10 and that Γ_f is equal to two- or three-tenths of an eV, while Γ_d is equal to 2 or 3 eV. We will use this estima-

tion of the parameters when applying the theoretical model to the case of actinides.

To compute the average numbers of d and f electrons, we have to derive the usual self-consistent equations. The occupation numbers are given by

$$n_{d\sigma} = -\frac{1}{\pi}\,\mathrm{Im}\int_{-\infty}^{E_F} G^{\sigma}_{dd}(E)\,dE\,, \tag{25a}$$

$$n_{f\sigma} = -\frac{1}{\pi}\,\mathrm{Im}\int_{-\infty}^{E_F} G^{\sigma}_{ff}(E)\,dE\,. \tag{25b}$$

We give the results of the calculation as a function of $n_\sigma = n_{d\sigma} + n_{f\sigma}$ and of $n_{d\sigma} - n_{f\sigma}$:

$$n_{d\sigma} + n_{f\sigma} = n_{1\sigma} + n_{2\sigma}\,, \tag{26a}$$

$$n_{d\sigma} - n_{f\sigma} = A(n_{1\sigma} - n_{2\sigma}) + \frac{B}{\pi}\ln\left(\frac{\Gamma_2}{\Gamma_1}\,\frac{\sin\pi n_{1\sigma}}{\sin\pi n_{2\sigma}}\right)\,. \tag{26b}$$

The occupation numbers $n_{1\sigma}$ and $n_{2\sigma}$ are

$$n_{1\sigma} = \frac{1}{\pi}\cot^{-1}\frac{E_{10} + Un_{-\sigma}}{\Gamma_1}\,, \tag{27a}$$

$$n_{2\sigma} = \frac{1}{\pi}\cot^{-1}\frac{E_{20} + Un_{-\sigma}}{\Gamma_2}\,, \tag{27b}$$

with

$$E_{10} = E_1^{(0)} - E_F\,, \tag{28a}$$

$$E_{20} = E_2^{(0)} - E_F\,. \tag{28b}$$

The coefficients A and B are independent of the spin and are given by

$$A = \frac{(E_d^{(0)} - E_f^{(0)})(E_1^{(0)} - E_2^{(0)}) + (\Gamma_d - \Gamma_f)(\Gamma_1 - \Gamma_2)}{|Z|}\,, \tag{29a}$$

$$B = \frac{(E_d^{(0)} - E_f^{(0)})(\Gamma_1 - \Gamma_2) - (\Gamma_d - \Gamma_f)(E_1^{(0)} - E_2^{(0)})}{|Z|}\,. \tag{29b}$$

So Eqs. (26), using Eqs. (27)–(29) and also (21)–(23), give four self-consistent equations for $n_{d\uparrow}$, $n_{d\downarrow}$, $n_{f\uparrow}$, and $n_{f\downarrow}$ which give the values of these four numbers. In principle, we obtained, by integration from $-\infty$ to E_F, only the occupation numbers at $T=0$; but since Γ_f is much larger than kT at room temperature in actinides, and *a fortiori* so are Γ_d, Γ_1, and Γ_2, the effect of temperature will be small and we will not consider it here.

The set of self-consistent equations can be practically computed easily by first taking Eq. (26a), which gives n_σ as a function of $n_{-\sigma}$:

$$n_\sigma = \frac{1}{\pi}\cot^{-1}\frac{E_{01} + Un_{-\sigma}}{\Gamma_1} + \frac{1}{\pi}\cot^{-1}\frac{E_{02} + Un_{-\sigma}}{\Gamma_2}\,. \tag{30}$$

We shall first solve Eq. (30) and then put n_σ and $n_{-\sigma}$ in Eq. (26b) to directly compute $n_{d\sigma}$ and $n_{f\sigma}$, because the difference $n_{d\sigma} - n_{f\sigma}$ depends only on $n_{-\sigma}$, for a fixed position of the d and f levels.

It is also interesting to note that, if $n_{f\uparrow} \neq n_{f\downarrow}$, we have automatically $n_{d\uparrow} \neq n_{d\downarrow}$, because of the peculiar form of the self-consistent equations and especially of the approximation (7) used here. So the research of the magnetic solutions of Eq. (30) gives all the magnetic solutions of the system (26). So the approximation (7) gives simplifications in handling mathematically the equations, without altering too much the physical results.

IV. DISCUSSION OF MAGNETIC SOLUTIONS

We discuss the different possible solutions of the set (26) of self-consistent equations, and we are especially interested in the possibility of magnetic solutions according to the different values of the parameters. There are six parameters Γ_f, Γ_d, U, V_{df}, and the relative positions of the d and f levels compared to the Fermi level, i.e.,

$$E_{0d} = E_d^{(0)} - E_F\,, \quad E_{0f} = E_f^{(0)} - E_F\,.$$

In fact, there are five dimensionless parameters obtained by dividing five parameters by the last one, for example, U. So in general the discussion is very long, but we are interested in the application of our results to the physical case of pure actinides. We shall consider that the actinide series is described by the filling up of the $5f$ shell, so that E_{0f} decreases from large positive values to negative values along the series. On the contrary, the position E_{0d} of the atomic $6d$ level will be considered here to remain constant with a positive value in order that the occupation number n_d be relatively small compared to 1 in the actinide series. Thus the only considered case corresponds to $E_{0d} > 0$, and the case $E_{0d} < 0$ will not be studied here. Also, the ratio Γ_d/Γ_f can be taken much greater than 1 and constant in the actinide series.

Therefore, we first study in detail the different solutions inside the classical Anderson diagram according to the relative values of $\pi\Gamma_f/U$ and E_{0f}/U for fixed E_{0d}, V_{df}, and Γ_d/Γ_f values (Sec. IV A) and then we discuss the occurrence of magnetic solutions when we make varying V_{df}, Γ_d/Γ_f, and E_{0d} (Sec. IV B).

A. Anderson Diagram (E_{0f}/U, $\pi\Gamma_f/U$) for Self-Consistent Equations

The classical method of solving Eq. (30) consists in plotting $n_\uparrow$ as a function of $n_\downarrow$ and then $n_\downarrow$ as a function of $n_\uparrow$; the points of intersection of the two obtained curves are the solutions of Eq. (30). There always exists a nonmagnetic solution $n_\uparrow = n_\downarrow = n_0$ given by

$$\pi n_0 = \cot^{-1}\frac{E_{01} + Un_0}{\Gamma_1} + \cot^{-1}\frac{E_{02} + Un_0}{\Gamma_2}\,. \tag{31}$$

n_0 increases continuously when E_{0f} decreases from $+\infty$ to $-\infty$ with a fixed E_{0d} value.

In some cases, there are one or several magnetic solutions $n_\uparrow \neq n_\downarrow$, in addition to the nonmagnetic solution. The solutions of the self-consistent equations are discussed in the classical Anderson plot in a plane with the coordinates E_{0f}/U and $\pi\Gamma_f/U$ for constant values of Γ_d/Γ_f, V_{df}, and E_{0d} (>0). Figure 6 shows the Anderson diagram for $\Gamma_d/\Gamma_f = 10$, $E_{0d} = \Gamma_d$, and $V_{df} = 0$.

We can distinguish several regions in Fig. 6: For E_{0f}/U roughly larger than 0 or smaller than -1 or also for U smaller than a critical value U_0, we obtain a nonmagnetic solution as in the Anderson case, either because the 5f level is almost completely empty or occupied, or because the strength of the Coulomb repulsion is too small. For E_{0f}/U between roughly 0 and -1 and for $U > U_0$, there is one magnetic solution as in the Anderson case. For E_{0f}/U close to 0 and $U > U_1$ on one side and for E_{0f}/U close to -1 and $U > U_2$ on the other side, we have two regions with two magnetic solutions, which is different from the nondegenerate case of Anderson.

The mathematical equations of the limiting curves separating the different regions of Fig. 6 are obtained as follows:

(i) The boundary curve of the magnetic region with one magnetic solution, i. e., the boundary between the nonmagnetic solution and the magnetic solution between U_1 and U_0 on one side and U_0 and U_2 on the other side, as well as the boundary between the magnetic region with one magnetic solution and the magnetic region with two magnetic solutions for U larger than U_1 or U_2, is given by the classical condition for the appearance of a magnetic solution from a nonmagnetic solution. Mathematically, this condition can be obtained by taking small variations $\delta n_\uparrow$ and $\delta n_\downarrow$ from a nonmagnetic solution n_0 given by (31) and by writing $\delta n_\uparrow = -\delta n_\downarrow \neq 0$. We obtain the classical condition

$$\frac{U}{\pi}\left(\frac{\sin^2\pi n_{10}}{\Gamma_1}+\frac{\sin^2\pi n_{20}}{\Gamma_2}\right)=1\ , \tag{32a}$$

or also, as usual,

$$U\rho_0(E_F)=1\ , \tag{32b}$$

where $\rho_0(E_F)$ is the extra d and f total density of states for one-spin direction.

(ii) The boundary curve between the magnetic region with two magnetic solutions and the nonmagnetic region for U larger than U_1 or U_2 is determined by another condition. One has to write down that two magnetic solutions appear together. In the nonmagnetic domain, the two curves $n_\uparrow(n_\downarrow)$ and $n_\downarrow(n_\uparrow)$ have only one intersection point, while in the magnetic domain with two magnetic solutions, the two curves have five intersection points. So the boundary is determined when the two curves $n_\uparrow(n_\downarrow)$ and $n_\downarrow(n_\uparrow)$ are tangent to each other in two points $n_{\uparrow 0}$ and $n_{\downarrow 0}$ corresponding to the magnetic solution $n_{\uparrow 0} \neq n_{\downarrow 0}$, as shown in Fig. 7. This condition is written, with obvious notations,

$$\frac{U^2}{\pi^2}\left(\frac{\sin^2\pi n_{1\uparrow 0}}{\Gamma_1}+\frac{\sin^2\pi n_{2\uparrow 0}}{\Gamma_2}\right)\times\left(\frac{\sin^2\pi n_{1\downarrow 0}}{\Gamma_1}+\frac{\sin^2\pi n_{2\downarrow 0}}{\Gamma_2}\right)=1\ , \tag{33a}$$

or

$$U^2\rho_{\uparrow 0}(E_F)\,\rho_{\downarrow 0}(E_F)=1\ . \tag{33b}$$

So when E_{0f} decreases from $+\infty$ to $-\infty$, we can have three different possible situations according to the different values of U.

(i) If $U < U_0$, the solution is always nonmagnetic, whatever the value of E_{0f}.

(ii) If $U_0 < U < U_1$ for the first transition encountered when E_{0f} decreases or if $U_0 < U < U_2$ for

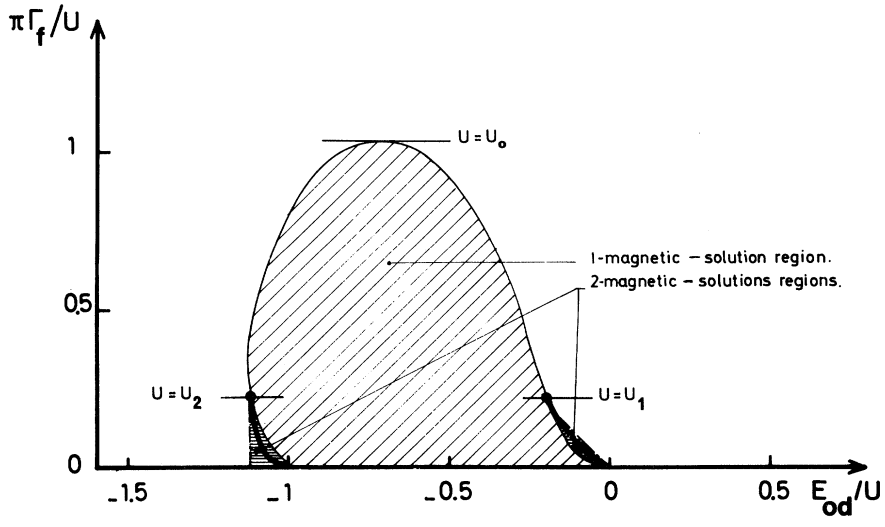

FIG. 6. Diagram of the self-consistent solutions in the plane ($\pi\Gamma_f/U$, E_{0f}/U) for $E_{0d} = \Gamma_d = 10\Gamma_f$, $V_{df} = 0$. Large hatching corresponds to the region with one magnetic solution; compact hatching corresponds to the regions with two magnetic solutions. The thin line corresponds to the boundary of the one magnetic solution region, the dashed line corresponds to the boundary between zero and two magnetic solutions regions, and the thick line gives the position of the first-order transition.

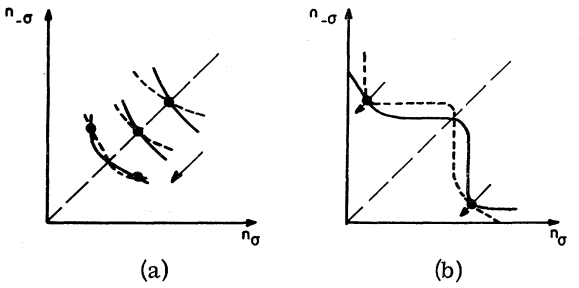

FIG. 7. Two cases for the appearance of magnetic solutions shown in a plot of $n_{-\sigma}$ vs n_σ: (a) appearance of one magnetic solution from one nonmagnetic solution [condition (32) in text], and (b) appearance of two magnetic solutions together [condition (33)].

the second transition encountered when E_{0f} decreases, the transitions from a nonmagnetic state to a magnetic state are always second-order ones and are given by the condition (32), as explained in the Appendix. The second-order transition line is given by the thin line.

(iii) If $U_1 < U$ for the first transition encountered when E_{0f} decreases or if $U_2 < U$ for the second transition encountered when E_{0f} decreases, one goes from a nonmagnetic solution to two possible magnetic solutions, and both the stable magnetic solution and the point where one goes from a nonmagnetic to a magnetic state are determined by the computation of the total energy as explained in the Appendix. From the calculation of the total energy, a first-order transition is found when going from the nonmagnetic region to the magnetic region by decreasing the E_{0f}/U value. The first-order transition line is given by the thick line in Fig. 6 or also Figs. 8 and 10. This line starts from $E_{0f} = 0$ and $E_{0f} = -U$ for infinite U values and reaches the second-order transition line at U equal to U_1 and U_2.

The first and second cases are similar to the classical case of Anderson which has been applied to transition impurities in noble metals.[34,36]. The third case is similar to the case of orbitally degenerate virtual bound states which has been applied to rare-earth metals and especially to the phase diagram of cerium metal.[33] Let us now discuss which case corresponds to the actinides series. The exact values of U_0, U_1, and U_2 depend on the parameters V_{df}, Γ_d/Γ_f, and E_{0d}, but for $V_{df} = 0$, we can say that U_0 is of order $\pi\Gamma_f$ while U_1 and U_2 are of order $\pi\Gamma_d$ and, as will be studied in detail later on, the effect of V_{df} is to increase the values of U_0, U_1, and U_2. Physically, we can understand the difference between the two cases by comparing the relative importance of the "f magnetic moment" $(n_{f\uparrow} - n_{f\downarrow})$ and the "d magnetic moment" $(n_{d\uparrow} - n_{d\downarrow})$ which always exist together because of the peculiar form of the self-consistent equations. For the case studied here of $E_{0d} > 0$ and $V_{df} = 0$, the f magnetic moment is generally much larger than the d magnetic moment. At the magnetic transition, it appears essentially an f magnetic moment, but the order of the transition in the Hartree-Fock approximation is determined by the relative importance of the d magnetic moment compared to the f magnetic moment, as already explained in the similar case of a twofold orbitally degenerate virtual bound state.[33] Moreover, the importance of the d magnetic moment is essentially dominated by the importance of the ratio $\pi\Gamma_d/U$.

Thus two cases can be considered: If U is smaller than $\pi\Gamma_d$, the d magnetic moment is very small and the transition is a second-order one as if the two levels $f\uparrow$ and $f\downarrow$ were alone exactly as in the nondegenerate virtual-bound-state case of Friedel and Anderson.[34,36] On the contrary, if U is larger than $\pi\Gamma_d$, the d magnetic moment is important and the transition is a first-order one because the variations of the occupation numbers $n_{d\uparrow}$ and $n_{d\downarrow}$ are important at the magnetic transition, exactly as in the twofold orbitally degenerate virtual-bound-state case applied previously to rare-earth metals.[33]

In actinide series, to our knowledge, the magnetic moment, when it appears, has only an f character. So in this theoretical model, we have to consider that the d magnetic moment is negligible and consequently that $\pi\Gamma_f < U < \pi\Gamma_d$. Consequently, we are in the case $U_0 < U < U_1$ and $U_0 < U < U_2$ and the transitions are always second-order ones. As far as we know in the present experimental situation, the first-order transitions obtained in this Hartree-Fock approximation have no physical meaning, in contrast to the case of rare earths.

At last, from the above discussion, we can also conclude that, since the d magnetic moment remains always small in the interesting physical case, the relative importance of the different parameters U_{dd}, U_{ff}, U_{df}, and J_{df} has not a real physical importance, which justifies the approximation (7).

B. Discussion of Self-Consistent Equations with V_{df}, Γ_d/Γ_f, and E_{0d}

The effect of the hybridization term V_{df} is clearly shown in Fig. 8, showing the magnetic diagram $(\pi\Gamma_f/U,\ E_{0f}/U)$ for different V_{df} values, and in Fig. 9, showing the plot of the occupation numbers $n_{f\sigma}$ and $n_{d\sigma}$ vs E_{0f}/U for different values of V_{df} and U. In Fig. 9, we can observe the nonmagnetic domains for large positive or large negative E_{0f}/U values and the magnetic domain between them. We have also chosen two different U values, one smaller than U_1 and U_2 and giving second-order transitions for $V_{df} = 0$ and the other one larger than U_1 and U_2

and giving first-order transitions for $V_{df}=0$. We can notice that for a small U value ($U=0.5\Gamma_d$) the f magnetic moment is much larger than the d magnetic moment in the magnetic domain, while for a large U value ($U=2\Gamma_d$) the d magnetic moment can be of the same order as the f magnetic moment. So clearly the case of a large U value giving rise to first-order transitions has to be avoided for describing the experimental situation of actinides series with the theoretical model, as was already pointed out.

When E_{0f} goes from $+\infty$ to $-\infty$, $n_{f\sigma}$ varies from 0 to 1 and $n_{d\sigma}$ varies from n_{d0} to n_{d1} ($n_{d1}<n_{d0}$), given by

$$n_{d0}=\frac{1}{\pi}\cot^{-1}\frac{E_{0d}+Un_{d0}}{\Gamma_d}\,,$$
$$n_{d1}=\frac{1}{\pi}\cot^{-1}\frac{E_{0d}+U+Un_{d1}}{\Gamma_d}\,. \tag{34}$$

Finally, the effect of V_{df} shown in Figs. 8 and 9 can be summarized as follows.

(i) The increase of V_{df} gives an increase of the critical values U_0, U_1, and U_2 and leads to a general "collapse" of the magnetic domain on the axis E_{0f}/U, as shown in Fig. 8. Consequently, the magnetic domain decreases as shown in both Figs. 8 and 9. Moreover, the transitions become smoother with increasing V_{df} values because of the increase of U_1 and U_2; on the right-hand side of Fig. 9, we see that the magnetic transitions which are first-order one at $V_{df}=0$ become second order and at last disappear with increasing V_{df} values.

(ii) The increase of V_{df} gives also a shift of the magnetic domain toward larger E_{0f} values, which physically corresponds to the relative removing of the two hybridized levels E_1^σ and E_2^σ.

(iii) A strong d-f hybridization tends to bring the numbers $n_{d\sigma}$ and $n_{f\sigma}$ closer to each other. This effect is observed on the variation of $n_{d\sigma}$ vs E_{0f}, which presents a maximum for large V_{df} values, while it decreases regularly from n_{d0} to n_{d1} for zero or small V_{df} values.

(iv) At a fixed E_{0f} value, the numbers of electrons $n_{d\sigma}$ and $n_{f\sigma}$ are generally rapidly increased by the hybridization as shown in Fig. 9. Moreover, although the magnetic domain is moved toward larger E_{0f} values, the total number of d and f electrons increases generally at the first magnetic transition. This effect will be described later on in detail and used for describing actinide metals.

We have taken till now a constant ratio Γ_d/Γ_f much larger than 1. It is interesting to show that changing the ratio Γ_d/Γ_f modifies only slightly the physical results. The magnetic diagram is shown in Fig. 10 according to different Γ_d/Γ_f values varying from 1 to $+\infty$, in the case of a zero V_{df} value. The limiting case $\Gamma_d/\Gamma_f\to\infty$ corresponds to an Anderson diagram shifted along the E_{0f}/U axis by the quantity $(1/\pi)\cot^{-1}(E_{0d}/\Gamma_d)$, which is simply the number of d electrons found as constant in this limit whatever the E_{0f} value. In this limit, the transitions are obviously always second-order ones as in Anderson case.

Finally, we can discuss very briefly the influence of E_{0d}. We have not treated here the case $E_{0d}<0$, because it corresponds physically to the case of a large d magnetic moment. For $E_{0d}>0$, the effect of E_{0d} is essentially to shift along the E_{0f}/U axis the magnetic diagram with respect to the magnetic diagram of the classical Anderson case by a quantity of the order of the number of d electrons. This is shown in Fig. 8, where we can compare the magnetic domain for $E_{0d}=\Gamma_d$ to the magnetic domain in the Anderson case for $E_{0d}\to+\infty$. Since the variation of n_d is small when we make varying E_{0d} around a mean positive value—for example, $E_{0d}=\Gamma_d$—the physical results are not deeply changed by a not too large variation of E_{0d}.

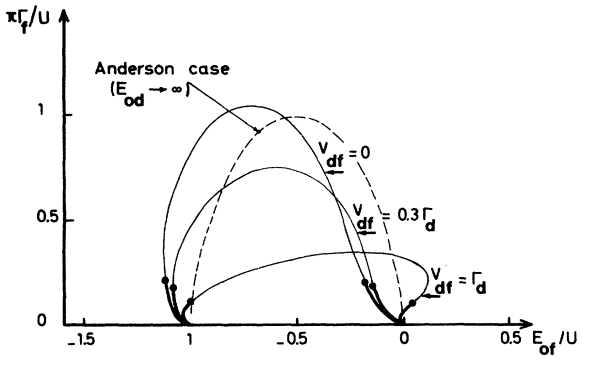

FIG. 8. Effect of V_{df} ($V_{df}=0$, $0.3\Gamma_d$, Γ_d) on the magnetic diagram ($\pi\Gamma_f/U$, E_{0f}/U) for $E_{0d}=\Gamma_d=10\Gamma_f$. The dashed line corresponds to the simple one virtual-bound-state Anderson case. The thick line is the first-order transition and the thin line the second-order one.

V. APPLICATION TO PURE ACTINIDES

In Secs. II–IV, we have developed a model for one impurity with two d and f virtual bound states. Now we apply our results to the case of pure actinides by making the crude approximation which considers the actinide metals as a collection of such independent impurities. This approximation gives certainly a too simplified picture for actinides where the band character of 6d and 5f electrons is important, but it is not too bad, because in the study of magnetic properties the main effect comes from the density of states.

To compare our theoretical results to experimental data, we have to identify each actinide and to choose the values of the different parameters, in the following way.

(i) Each actinide is identified by its total number

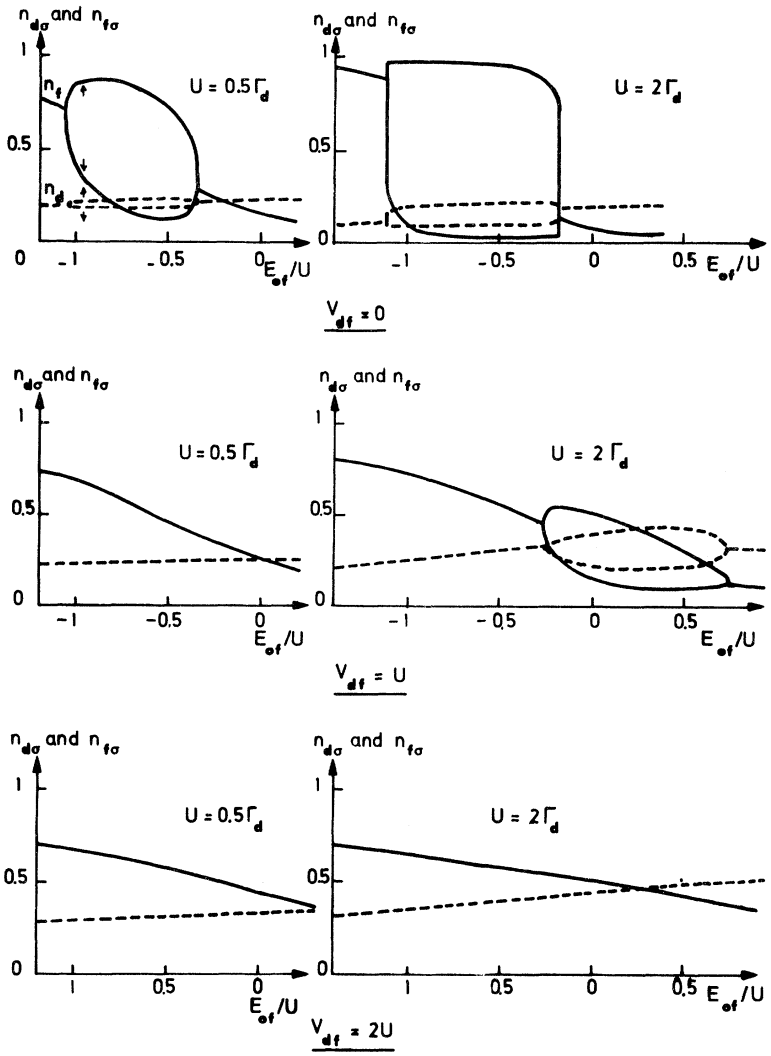

FIG. 9. Plot of $n_{f\uparrow}$ and $n_{f\downarrow}$ (full line) and $n_{d\uparrow}$ and $n_{d\downarrow}$ (dashed line) vs E_{0f}/U for $E_{0d} = \Gamma_d = 10\Gamma_f$ and for two U values: $U = 0.5\Gamma_d$ (left-hand side) and $U = 2\Gamma_d$ (right-hand side). The effect of V_{df} is shown by choosing three values: $V_{df} = 0$, $V_{df} = U$, $V_{df} = 2U$.

of $7s$, $6d$, and $5f$ electrons which increases along the series from 3 in actinium to 11 in berkelium. In our simplified model, which does not take into account the orbital degeneracy, the total number of d and f electrons is simply given by

$$N = 5\sum_\sigma n_{d\sigma} + 7\sum_\sigma n_{f\sigma} . \tag{35}$$

The number of conduction electrons or $7s$ electrons is taken to be constant and equal to 2. So, along the series, E_{0f} decreases regularly and N increases continuously in order to fit the integer values of each actinide, from 1 for actinium to 9 for berkelium. For each actinide, we can define a spin magnetic moment given by its projection along the z axis (in the Hartree-Fock approximation):

$$M = 5\,(n_{d\uparrow} - n_{d\downarrow}) + 7\,(n_{f\uparrow} - n_{f\downarrow}) . \tag{36}$$

M is expressed in (36) in Bohr-magneton units.

In a similar way, we can define the total density of d and f states from the expressions (17) by the formula

$$\rho_{df\sigma}(E_F) = 5\rho_{d\sigma}(E_F) + 7\rho_{f\sigma}(E_F) . \tag{37}$$

(ii) As already deduced from the comparison between Figs. 3 and 5, the ratio Γ_d/Γ_f can be taken of order 10, Γ_f of order $\frac{2}{10}$ or $\frac{3}{10}$ eV, and Γ_d of order 2 or 3 eV in the actinide series, in order to make the virtual-bound-state model consistent with band parameters. In the following, we take $\Gamma_f = 0.2$ eV and $\Gamma_d = 2$ eV, and we have to notice that changing slightly the Γ_d and Γ_f values around these values does not affect the physical results, as shown in Sec. IV.

(iii) Other parameters which can be chosen together are the position E_{0d} of the $6d$ level and the U value. We had first assumed that the position of the $6d$ level does not vary along the actinide series. There are relatively many ways of determining E_{0d} U by fitting some of the experimental data of acti-

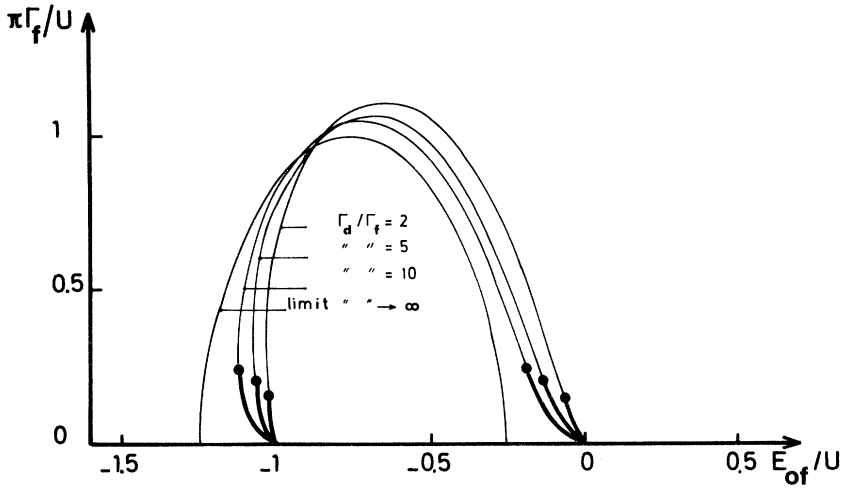

FIG. 10. Effect of changing Γ_d/Γ_f value ($\Gamma_d/\Gamma_f = 2$, 5, 10, ∞) on the magnetic diagram ($\pi\Gamma_f/U$, E_{0f}/U) for $E_{0d} = \Gamma_d$, $V_{df} = 0$ and with same notations as in Fig. 9.

nides, but the most quantitative way is certainly to fit the experimentally expected numbers of d electrons by the theoretical expressions (34), which give $n_{d\sigma}$ at the beginning and the end of the series. Since the number of d electrons is equal to 2 at the beginning of the series for thorium and equal to 1 for berkelium, the expressions (34) lead approximately to the very simple choice of parameters $E_{0d} = U = \Gamma_d$.

This choice is also consistent with remarks

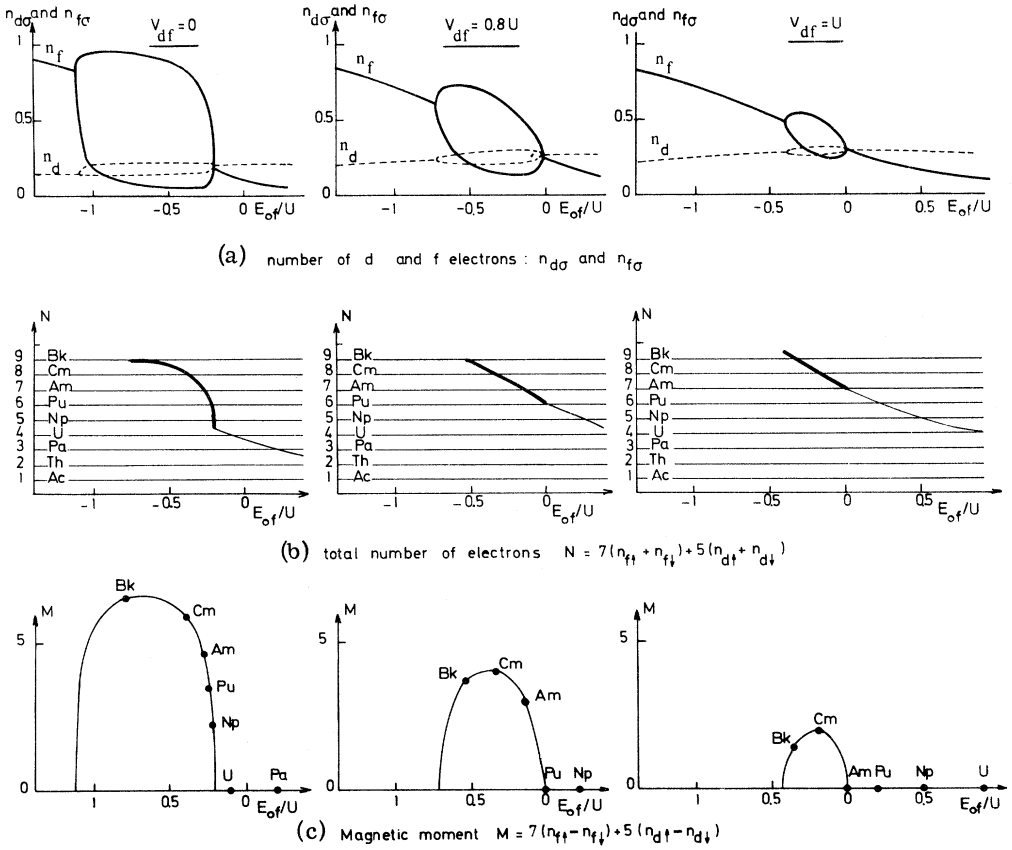

FIG. 11. Plot of (a) $n_{d\sigma}$ and $n_{f\sigma}$, (b) the total number N of d and f electrons, and (c) the magnetic moment M in Bohr magnetons vs E_{0f}/U for three different V_{df} values ($V_{df} = 0$, $0.8U$, U). The choice of the other parameters and the identification of each actinide is explained in the text.

which have been previously made. This chosen value of E_{0d} by fitting $n_{d\sigma}$ gives the maximum of Γ_1 just at uranium when V_{df} is large. The agreement for the magnitude of the widths between Figs. 3 and 5 was obviously contained by definition in the choice of Γ_d and Γ_f, but the agreement for the position of the maximum width was not obvious and makes the model consistent with the results of Fig. 3.

Moreover, the chosen value of $U = \Gamma_d$ is satisfying because it leads to second-order transitions even for $V_{df} = 0$ and to a small d magnetic moment. The choice of a constant U value along the series is rather difficult to justify theoretically because on one side the atomic U_{ff} Coulomb integral increases along the series and on the other side the reduction of the atomic Coulomb repulsion by the correlations is not well known and certainly not constant along the series.[38,39] However, in our model we can also obtain the same physical results with a larger U value but then choosing a larger V_{df} value.

(iv) The last parameter is V_{df}, which is not well known and is again estimated by comparison with the band structure or experimental data. The comparison between Figs. 3 and 5 had previously indicated that V_{df} is certainly large in actinides and especially for U, Np, and Pu, in order to account for the known experimentally d-f hybridization. So here, after having chosen $U = \Gamma_d = 2$ eV, we take three typical values for V_{df}: $V_{df} = 0$, $V_{df} = 0.8U$, and $V_{df} = U$.

With the preceding values of the parameters, we have plotted in Fig. 11 the numbers $n_{f\sigma}$ and $n_{d\sigma}$ of f and d electrons, the total number N of d and f electrons given by (35), and the magnetic moment M given by (36), as a function of E_{0f}.

In Fig. 11, we see that, without hybridization, neptunium, plutonium, and americium would be magnetic, and magnetism would appear just after uranium, in a situation similar to that of rare earths, where magnetism appears at the beginning of the series. On the contrary, to account for the experimental situation, i. e., the observed "delay" in the appearance of magnetism which occurs only for elements after americium, we have to assume inside the present model a very strong d-f hybridization $V_{df} = U = 2$ eV.

However, in Fig. 11, for $V_{df} = U$, which is the chosen value for the strong hybridization, the values found theoretically for the magnetic moments are roughly $2\mu_B$, to be compared to the $8\mu_B$ experimental values for curium and berkelium.

Finally, Fig. 12 shows the plot of the different deduced values for the density of states for one-spin direction along the actinide series. The line labeled 1 gives the density of states deduced from the electronic constant of the specific heat, as reviewed by Lee *et al.*[1] The line labeled 2 gives the density of states deduced from the magnetic susceptibility assuming no exchange-enhancement factor, as reviewed by Brodsky.[3] The line labeled 3 gives the theoretical total density of states for one-spin direction taken as the sum of the d and f density of states given by (37) and of a 7s density of states estimated to 0.5 states/eV atom. In Fig. 12, we can see that an agreement is found between the experimental curve 1 and the theoretical curve 3. The satisfactory agreement between lines 1 and 3 is a direct consequence of the choice of the Γ_d and Γ_f parameters resulting from the work of Kmetko and Hill, but since the APW band calculations are inaccurate in describing the 5f bands, the agreement of Fig. 12 gives a new information beyond the work of Kmetko and Hill concerning the value of the density of states at the Fermi level. The discrepancy between lines 1 and 3 on one side and line 2 on the other side can perhaps be attributed to an exchange-enhancement effect with a factor of 2 or 3. Precise data on the density of states of plutonium and of the elements which follow it would be interesting for continuing the comparison with the theoretical model.

VI. CONCLUSION

In conclusion, the simple model of two hybridized and nondegenerate d and f virtual bound states can first be made consistent with previous band calculations and with the experimental data, giving a large density of states at the Fermi level and then can account satisfactorily for the occurrence of localized magnetism only in the middle of the series after americium. But the experimentally observed change, from the d-f hybridized metals such

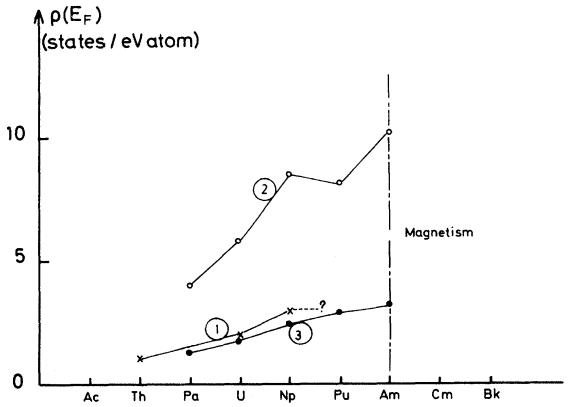

FIG. 12. Plot of the total density of states at Fermi level $\rho(E_f)$ (in states/eV atom) for nonmagnetic actinides, as explained in the text: 1) (×) is deduced from specific-heat data, 2) (○) from magnetic susceptibility data, 3) (●) from theoretical calculation with same parameters as in Fig. 11 and $V_{df} = U$.

as Pa, U, Np, and Pu to the magnetic rare earths like metals such as Cm and Bk, which occurs around Am is much more abrupt and rapid than the slow theoretical change, as can be seen either in the variation of the f bandwidth by comparison of Figs. 3 and 5 or in the high values of the Cm and Bk magnetic moments.

The theoretical too smooth change around americium is directly connected to some of our approximations: the constancy of V_{df} and U values along the series, and the Lorentzian shape of the d virtual bound state. A less-smooth shape of the d density of states such as that of a narrow band without tails or that of a "hyperbolic" virtual bound state[38] which decreases much more rapidly than the Lorentzian function, would improve the physical picture of actinides.

The theoretical model does not consider the orbital degeneracy and the spin-orbit coupling. The orbital degeneracy is important only for the description of magnetic elements. In the case of magnetic metals (in the middle of the f series as is gadolinium), curium has only a spin magnetic moment well described by (36), but berkelium has a spin and orbital magnetic moment which can be described only by taking into account the orbital degeneracy, in a model similar to that previously used for rare earths.[33] In the case of alloys with actinides impurities, plutonium and neptunium impurities are often magnetic, and neptunium appears generally more magnetic than plutonium,[3] which is clearly connected to the orbital degeneracy of the 5f level.

The spin-orbit coupling is very important physically for actinides, where it is of the order of 1 eV.[18] A spin-orbit coupling which is larger than Γ_f splits the 5f level into a $j=\frac{5}{2}$ level which is filled up till americium and a $j=\frac{7}{2}$ level which is filled up after americium. Physically, the hybridization is important for the first series corresponding to the filling of the $j=\frac{5}{2}$ level, because the d character is sufficiently large, while it becomes relatively small in the second series, which is very close to the rare-earth series. In this new approach, americium should not be magnetic, probably not because the density of states for the unique 5f level is too small to satisfy the condition (32), but more exactly because the $j=\frac{5}{2}$ level is almost completely filled up and the other one almost empty. This improvement of the model has been developed with more details elsewhere,[40] and it leads to a better agreement with the experimentally observed values of the magnetic moments for curium and berkelium.

A very natural application of our model is the study of alloys with actinides impurities, and in particular, as discussed elsewhere,[40] the superconductivity of lanthanum-based alloys with actinides impurities. The decrease of the superconducting transition temperature of lanthanum with small amounts of actinide impurities[41] has been experimentally found to be very small for thorium and uranium, very large for neptunium and plutonium with a maximum at neptunium, and at last very small for americium. So neptunium and plutonium impurities are magnetic in lanthanum, which is checked by the occurrence of a Kondo effect for La-Pu alloys[42] or also by magnetic moment experiments,[43] while the other impurities are not magnetic. This behavior can be qualitatively explained by taking into account in a very simplified way the spin-orbit coupling[40] and by considering the filling up of a $j=\frac{5}{2}$ level widely separated from the empty $j=\frac{7}{2}$ level by a large spin orbit, which leads to a nonmagnetic americium. Moreover, the effect of V_{df} is much smaller because the d character of lanthanum is smaller than in pure actinides, which leads to magnetic neptunium and plutonium impurities. So the superconductivity of lanthanum actinide, which has already been reported briefly,[40] supports the two ideas of a large spin-orbit coupling and of hybridization increasing with the d character.

Therefore, the model presented here can account for the "delay" in the occurrence of magnetism in actinides, and further work is in progress in the directions mentioned in the conclusion to improve the description of actinides.

ACKNOWLEDGMENTS

We are indebted to Dr. A. J. Freeman and Dr. H. H. Hill for giving us their data prior to publication.

APPENDIX: DETERMINATION OF ORDER OF NONMAGNETIC-MAGNETIC TRANSITION

The order of the transition from the nonmagnetic state to the magnetic state and also the E_{0f} value where magnetism appears are determined by the calculation of the total energy of the system.

The energy of d and f electrons is

$$\mathcal{E}_0=\sum_\sigma \int_{-\infty}^{E_F} E\,\rho_\sigma(E)\,dE - U n_\uparrow n_\downarrow . \tag{A1}$$

In the expression (A1), we have subtracted the Coulomb repulsion, according to the Koopman theorem. But here we are studying the problem of one actinide impurity in the presence of the conduction band. So the system of f and d electrons localized on the actinide impurity is not isolated and linked to the system of conduction electrons. In order to keep the total number of electrons constant, we have to take into account the transfer of localized electrons into the conduction band just at the Fermi energy E_F. So the thermodynamical potential to be minimized is

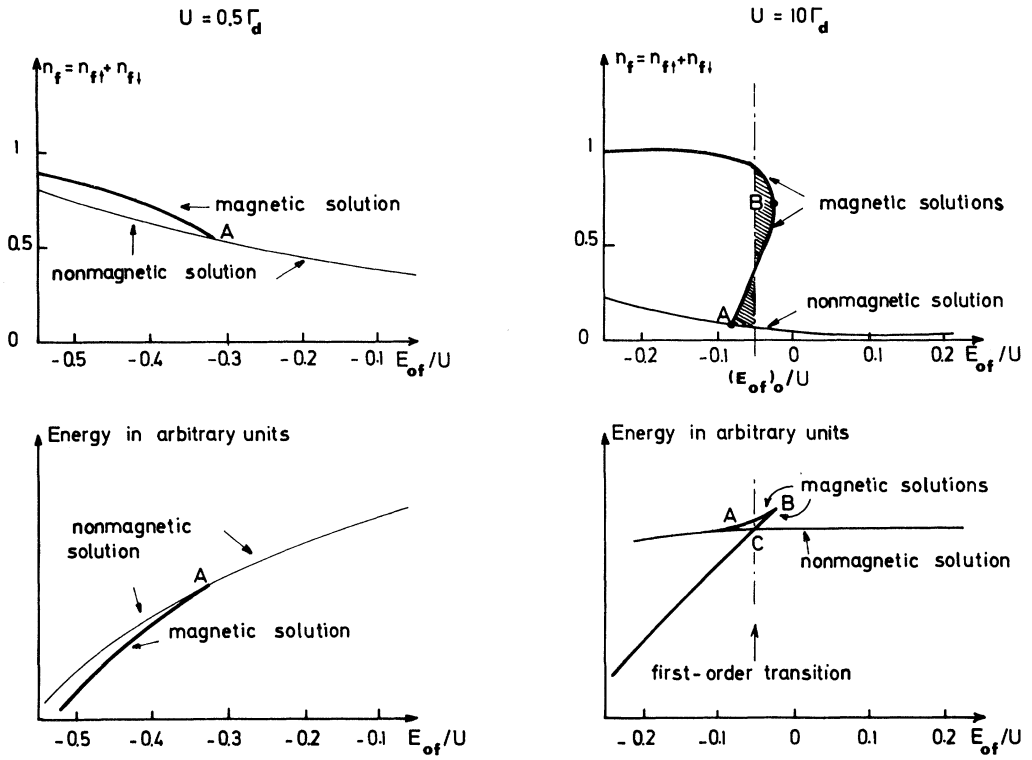

FIG. 13. Plot of the number of f electrons $n_f = n_{f\uparrow} + n_{f\downarrow}$ (top of the figure) and of the energy in arbitrary units (bottom of the figure) for $E_{0d} = \Gamma_d = 10\Gamma_f$, $V_{df} = 0$, and two different U values: $U = 0.5\Gamma_d$ (on the left-hand side) and $U = 10\Gamma_d$ (on the right-hand side) vs E_{0f}/U. The thin line corresponds to the nonmagnetic solution, the thick line to the magnetic solution, A to the condition (32), B to the condition (33). On the left-hand side, there is a second-order transition in A, and on the right-hand side there is a first-order transition in C for $E_{0f} = (E_{0f})_0$.

$$\mathcal{E} = \mathcal{E}_0 - NE_F = \sum_\sigma \int_{-\infty}^{E_F} (E - E_F)\rho_\sigma(E)\,dE - U n_\uparrow n_\downarrow , \tag{A2}$$

where

$$N = \sum_\sigma (n_{d\sigma} + n_{f\sigma}) . \tag{A3}$$

Making the same calculation as previously done for rare earths,[33] we obtain

$$\mathcal{E} = E_{01}\sum_\sigma n_{1\sigma} + E_{02}\sum_\sigma n_{2\sigma} + U n_\uparrow n_\downarrow - \frac{\Gamma_1}{\pi}\sum_\sigma \ln\left(\frac{G}{\Gamma_1}\sin\pi n_{1\sigma}\right) - \frac{\Gamma_2}{\pi}\sum_\sigma \ln\left(\frac{G}{\Gamma_2}\sin\pi n_{2\sigma}\right) . \tag{A4}$$

In the expression (A4), we have introduced a cutoff energy G always much larger than Γ_1 and Γ_2, corresponding to the bottom of the conduction band, in order to avoid the unphysical divergence due to the Lorentzian shape of the density of states as previously explained.[33]

It is easy to show that, when E_{0d} and E_{0f} are both varying, the total differential of $\mathcal{E}$, either obtained directly from the derivation of the Hamiltonian (1) itself or computed from the derivation of (A4), is given by

$$d\mathcal{E} = n_f\,dE_{0f} + n_d\,dE_{0d} , \tag{A5}$$

where n_f and n_d are, respectively, the number of the f and d electrons:

$$n_f = n_{f\uparrow} + n_{f\downarrow} , \quad n_d = n_{d\uparrow} + n_{d\downarrow} . \tag{A6}$$

So the result obtained for one virtual bound state[33] is easily extended to the case of two virtual bound states. If E_{0d} is fixed and only E_{0f} variable, the derivative of the total energy with respect to E_{0f} is equal to the total number of f electrons:

$$\frac{d\mathcal{E}}{dE_{0f}} = n_f = \sum_\sigma n_{f\sigma} . \tag{A7}$$

So in order to have the transition from nonmagnetism to magnetism, we have to plot n_f and $\mathcal{E}$ as a function of E_{0f} around the conditions (32) and (33) as shown in Fig. 13 for typical parameters: Either U is smaller than U_1, there is no magnetic region with two magnetic solutions, and the magnetic solution is always the most stable one, the transition is a second-order one given by the condition (32), as in the Anderson case. Or U is larger than U_1,

the typical plot of n_f and $\mathcal{S}$ is shown in Fig. 13 on the right-hand side. The points A and B given, respectively, by the conditions (32) and (33) correspond to changes of the sense of variation for E_{0f} and are turn points of the curve of $\mathcal{S}$ vs E_{0f}. The transition is a first-order one at the position $(E_{0f})_0$ shown in Fig. 13 and the two areas separated by the $n_f(E_{0f})$ curve and the value of $(E_{0f})_0$ are equal in Fig. 13, as previously explained for rare-earth metals.[33]

The E_{0f} value of the point A for the second-order transition and the $(E_{0f})_0$ value for the first-order transition are described by the thin and thick lines, respectively, in Figs. 6, 8, and 10.

---

*Part of Doctorat d'Etat thesis to be submitted by R. Jullien to the Faculté des Sciences d'Orsay.

†Supported by Consiglio Nazionale delle Ricerche, Roma.

‡Laboratoire associé au CNRS.

[1]J. A. Lee, P. W. Sutcliffe, D. J. Martin, and K. Mendelssohn, Proceedings of the Metallurgical Society A.I.M.E., Santa Fe, N. M., 1970, edited by W. N. Miner (unpublished), p. 58, and references therein.

[2]H. H. Hill, Physica 55, 186 (1971).

[3]M. B. Brodsky, in Proceedings of the Conference on Rare Earths and Actinides, Durham, 1971 (unpublished), p. 75, and references therein.

[4]J. A. Lee, in Ref. 3, p. 51, and references therein.

[5]H. H. Hill, in Ref. 1, p. 2, and references therein.

[6]J. Friedel, CEA Report No. 766, 1958 (unpublished).

[7]S. A. Marei, thesis (University of California, Berkeley, 1965) (unpublished) [UCRL Report No. 11984 (unpublished)].

[8]J. R. Peterson, J. A. Fahey, and R. D. Baybarz, in Ref. 1, p. 20.

[9]D. D. Koelling and A. J. Freeman, Solid State Commun. 9, 1369 (1971).

[10]W. R. Decker and D. K. Finnemore, Phys. Rev. 172, 430 (1968).

[11]J. L. Olsen, E. Bucher, M. Levy, J. Muller, E. Corenzwit, and T. Geballe, Rev. Mod. Phys. 36, 168 (1964).

[12]T. A. Sandenaw and R. B. Gibney, in Ref. 1, p. 68.

[13]A. J. Arko and M. B. Brodsky, in Ref. 1, p. 364.

[14]F. Y. Fradin and M. B. Brodsky, Intern. J. Magnetism 1, 89 (1970).

[15]B. M. Bansal, thesis (unpublished) (University of California, Berkeley, 1966) [UCRL Report No. 16782 (unpublished)].

[16]H. W. Ross and D. J. Lam, Phys. Rev. 165, 617 (1968).

[17]J. Friedel, J. Phys. Chem. Solids 1, 175 (1956).

[18]E. A. Kmetko and H. H. Hill, in Ref. 1, p. 233.

[19]M. J. Mortimer, AERE (Harwell) Report (unpublished).

[20]W. E. Gardner and T. F. Smith, Phys. Rev. 154, 309 (1967).

[21]J. C. Ho, N. E. Phillips, and T. F. Smith, Phys. Rev. Letters 17, 694 (1966).

[22]W. H. Zachariasen, in *The Metal Plutonium*, edited by A. S. Coffinberry and W. N. Miner (University of Chicago Press, Chicago, 1961), p. 99.

[23]B. T. Matthias, W. H. Zachariasen, G. W. Webb, and J. J. Engelhardt, Phys. Rev. Letters 18, 781 (1967).

[24]S. C. Carniglia and B. B. Cunningham, J. Am. Chem. Soc. 77, 1502 (1955).

[25]D. R. Stephens, H. D. Stromberg, and E. M. Lilley, J. Phys. Chem. Solids 29, 815 (1968).

[26]B. B. Cunningham and J. C. Wallmann, J. Inorg. Nucl. Chem. 26, 271 (1964).

[27]E. S. Sarkisov, Dokl. Akad. Nauk SSSR 166, 627 (1966).

[28]B. D. Dunlap, M. B. Brodsky, G. M. Kalvius, and G. K. Shenoy, in Ref. 1, p. 331.

[29]D. B. McWhan, thesis (University of California, Berkeley, 1961) (unpublished) [UCRL Report No. 9695 (unpublished)].

[30]D. B. McWhan, B. B. Cunningham, and J. C. Wallmann, J. Inorg. Nucl. Chem. 24, 1025 (1962).

[31]D. D. Koelling, A. J. Freeman, and G. O. Arbman, in Ref. 1, p. 194.

[32]A. J. Freeman and D. D. Koelling, J. Phys. Radium (to be published).

[33]B. Coqblin and A. Blandin, Advan. Phys. 17, 281 (1968), and references therein.

[34]J. Friedel, Can. J. Phys. 34, 1190 (1956); Nuovo Cimento 52, 287 (1958).

[35]S. Alexander and P. W. Anderson, Phys. Rev. 133, A1594 (1964).

[36]P. W. Anderson, Phys. Rev. 124, 41 (1961).

[37]E. Galleani d'Agliano, R. Jullien, and B. Coqblin, in Ref. 3, p. 69.

[38]B. Coqblin and G. Toulouse, J. Phys. Chem. Solids 29, 463 (1968).

[39]J. R. Schrieffer and D. C. Mattis, Phys. Rev. 140, A1412 (1965).

[40]B. Coqblin, E. Galleani d'Agliano, and R. Julien, in Proceedings of the Conference on Superconductivity in d and f Band Metals, Rochester, 1971, edited by D. H. Douglas (unpublished), p. 154.

[41]H. H. Hill, J. D. G. Lindsay, R. W. White, L. B. Asprey, V. O. Struebing, and B. T. Matthias, Physica 55, 615 (1971).

[42]H. H. Hill, R. O. Elliott, and W. N. Miner, in Proceedings of the CNRS Colloquium, Paris-Grenoble, 1969 (unpublished).

[43]J. P. Gatesoupe and C. H. de Novion, Solid State Commun. (to be published); and in Ref. 3, p. 84.